The Evolution of Large-Scale Subsurface Flow Patterns in the Sun

R.S. Bogart[1], C.S. Baldner[1], S. Basu[2], O. Burtseva[3], I. González Hernández[3], D.A. Haber[4], F. Hill[3], R. Howe[5], K. Jain[3], R. Komm[3], M.C. Rabello-Soares[1,6], S. Tripathy[3]

[1]Stanford University; [2]Yale University; [3]National Solar Observatory; [4]University of Colorado; [5]University of Birmingham; [6]Universidade Federal de Minas Gerais

Ring-diagram analysis permits us to infer large-scale flow fields at the photosphere and down to depths of about 0.95 R. We present comparisons of the mean zonal and meridional velocity profiles determined from uniform analysis techniques applied to three observational data sets, those from the SDO/HMI and SOHO/MDI missions and the GONG project, over the last 18 years. We pay special attention to measurements obtained during the summer of 2010, when observations from all three observatories were available. We discuss systematic effects affecting the individual datasets in order to analyse evolution of global flows over the time scale of the solar cycle.

The HMI ring-diagram pipeline has been producing flow-field measurements for over two years. Typical inversions for a single location on a single "day" are shown in Fig. 1. Mapping the inverted values at different target depths, we produce flow maps in the Stonyhurst coordinate frame for each sampling interval. Averages over the first 2+ Carrington rotations observed by HMI of such maps are shown in the left set of panels in Fig. 2. The flow patterns are of course dominated by the differential rotation at the corresponding depth relative to the rotating Carrington frame, but the basic meridional circulation pattern is also clear. The remaining panels of Fig. 2 display the differences between this basic flow pattern and the averages of succesive sets of 3 Carrington rotations for the two-year observing period. Variations in the torsional oscillation signal in the separate hemispheres for example are evident, but we must be cautious in interpreting the results. Since these maps are in an (averaged) Stonyhurst frame, any systematic longitudinal variations, such as those appearing in the zonal flows at high latitudes with an annual peridiodicity, must certainly be artifacts of the analysis procedure.

The temporal behaviour of the mean near-surface meridional and zonal flows at the equator over two years of HMI data are shown in Fig. 3. There is a slight approximately annual variation in the meridional component, but it is not in phase with the latitude of disc center as might be expected. We see no evidence for an annual variation of the zonal flow such as have been seen at the ~5m/s level in the global-mode analysis of GONG data.

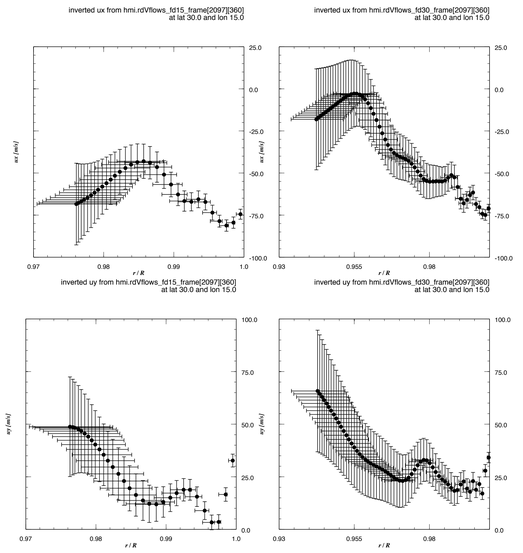

Fig. 1: Sample inversions for u_x (above) and u_y (below) of single tiles in the 15° (left) and 30° (right) HMI series. The large negative values of u_x are due to the fact that the regions (30° north in this case) are tracked at the Carrington rate, so the u_x measurement reflects the differential rotation profile in latitude as well as depth. Likewise, the positive values of u_y at this latitude reflect the poleward meridional flow.

In order to extend the evolutionary study backward over the longer time periods comprehended by GONG (since 2002) and MDI (samples from 1996–2010), we must characterize and understand any systematic differences from analysis of data from the various data sets. These can arise from differences in the analysis pipelines as well as the data themselves. We have compared flows from the three data sets during periods of contemporaneous observations, CR 2097–2111 for GONG and 2096–2098 for MDI. The GONG data were processed through an independent, but similar pipeline; only the inversions were identical. The MDI data were processed through the HMI pipeline, but with the regions tracked at a rate corresponding to the photospheric Doppler rotation rate for their central latitude rather than at the Carrington rate, meaning that each region samples a slightly different range of longitudes over its tracking interval. Also, the tracking intervals for HMI (1728 min) are slightly different from those for MDI and GONG (1664 min), owing to the different observing cadences. Comparisons of the mean zonal profiles of the meridional and zonal (after correction for tracking rates) flows are shown in Figs. 4 & 5.

Some features of the mean flows

The large-scale flows determined by ring-diagram analysis in the upper 14 Mm of the Sun are broadly consistent among MDI, GONG, and HMI contemporaneous measurements. There is, however, a 15–20 m/s offset in the zonal flows from MDI compared with those from GONG and HMI, with weak latitudinal dependence. It is evidently not due to differences in the tracking rate, as we have compared flows determined by tracking the MDI data at the Carrington rate as well as at differential rates (Fig 4c). There is markedly reduced scatter in the results for that case, which is likely due to the fact that with identical tracking rates the regions being compared are identical throughout the interval, not just at the midpoint; but the means are remarkably similar.

There is an asymmetric longitudinal variation in the measured zonal flow at the equator at depths of 7–14 Mm, with a strong effect near the eastern limb; it is consistent between HMI and GONG. Longitudinal asymmetries in the zonal flows seem to appear at high latitudes especially with an annual periodicity; these are undoubtedly due to a combination of projection effects and tracking. This also applies to the large meridional velocity components at high latitudes, which also exhibit an approximately annual periodicity.

The meridional circulation near the surface determined from HMI is slightly greater at middle latitudes and weaker at high latitudes than from MDI and GONG; but these differences (~5 m/s) are reversed at greater depths.

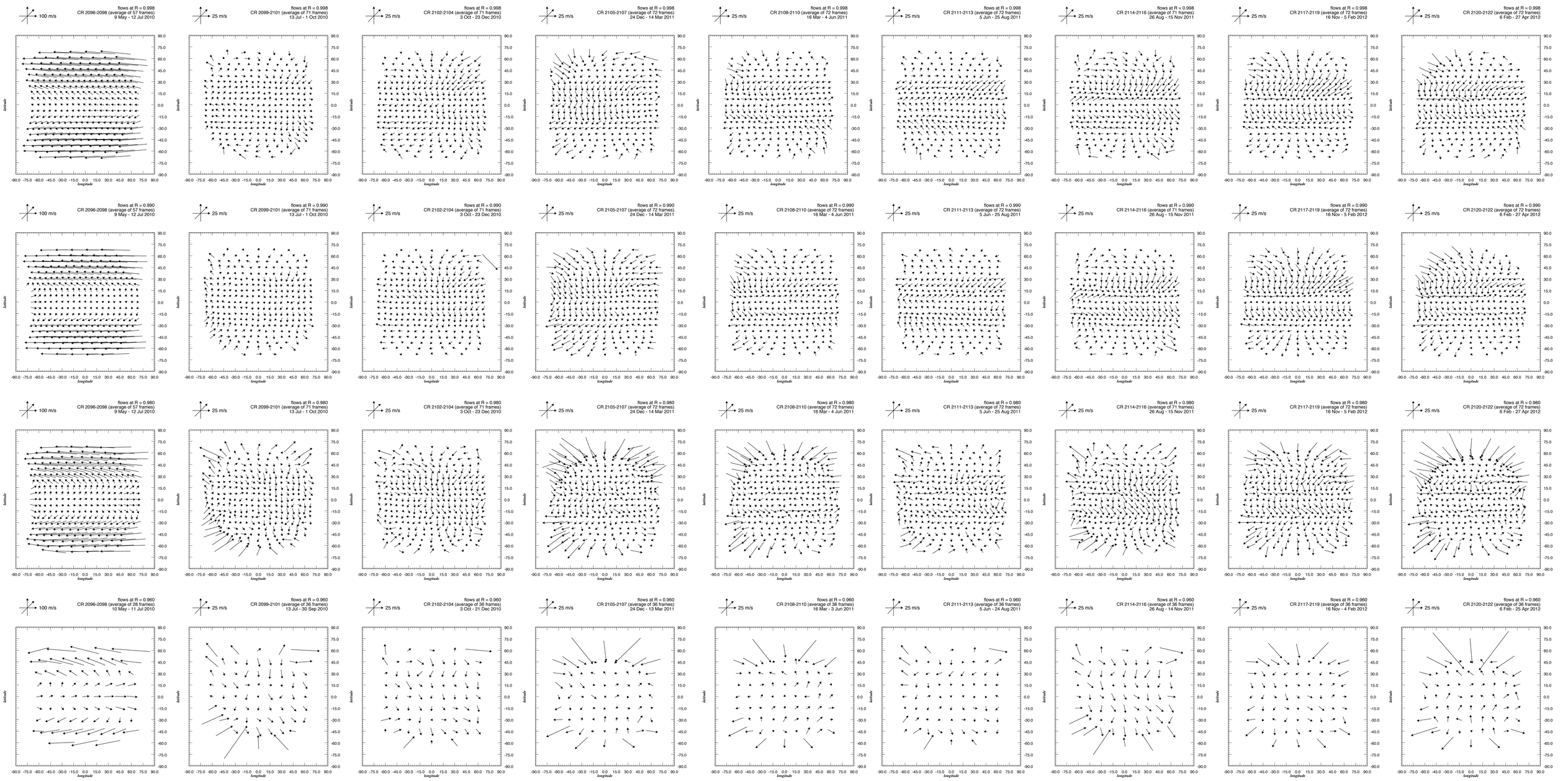

Fig. 2: Time variation of the mean flow fields at four depths, with each sample averaged over three Carrington rotations. The sampling depths are (top to bottom) 0.998, 0.99, 0.98, and 0.96 R; the first three are from analysis of 15° tiles, the last from 30° tiles. The panels on the left represent the absolute average flows (relative to the tile tracking at the Carrington rotation rate) over the first three Carrington rotations observed by HMI (2096–2098), and exhibit the basic differential rotation and meridional circulation at their respective depths. Successive sets of panel show the differences between the average of later sets of three Carrington rotations and the first set. The averages are taken at fixed heliographic latitudes and heliocentric (Stonyhurst) longitudes.

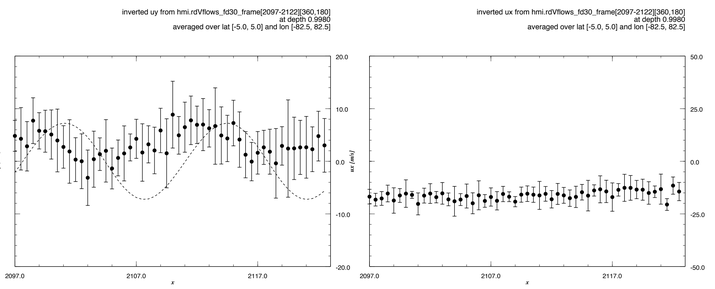

Fig. 3: Time variation of the mean near-surface meridional (left) and zonal (right) flows relative to the Carrington frame at the equator over two years. The dashed curve in the left is the B_0 angle.

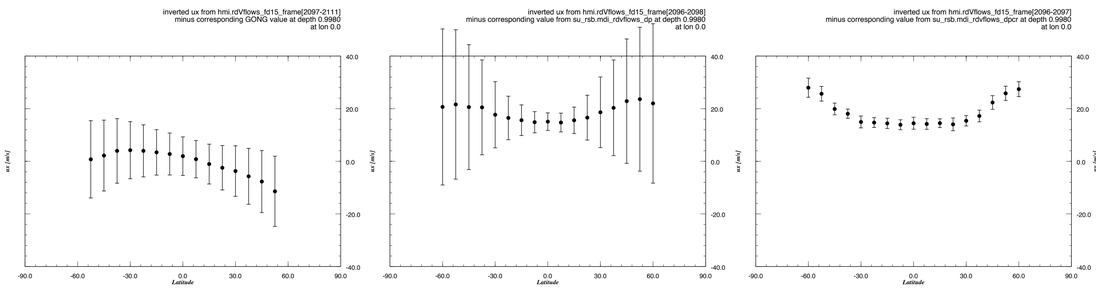

Fig. 4: Differences of the mean near-surface latitudinal zonal flow profile between HMI and (left) GONG and (middle) MDI over the same time intervals. The measurements have been corrected for the different tracking rates in the analyses. The plot on the right shows the differences between HMI and MDI when the MDI tiles are tracked at the Carrington rate like HMI.

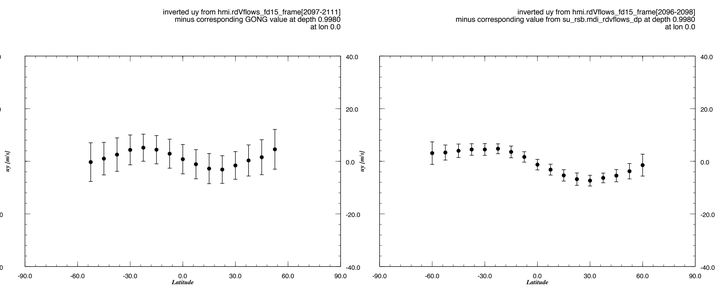

Fig. 5: Differences of the mean near-surface latitudinal meridional flow profile between HMI and (left) GONG and (right) MDI over the same time intervals.